A variable stiffness soft gripper with integrated ion-drag pump

Michael Smith, Krishna Manaswi Digumarti, Vito Cacucciolo, Herbert Shea

EPFL-LMTS, Switzerland

Citation: Michael Smith, Krishna Manaswi Digumarti, Vito Cacucciolo, Herbert Shea "A variable stiffness soft gripper with integrated ion-drag pump", Proceedings Volume PC12042, Electroactive Polymer Actuators and Devices (EAPAD) XXIV; PC120420A (2022)
doi: 10.1117/12.2615068

Event: SPIE Smart Structures + Nondestructive Evaluation, 2022, Long Beach, California, USA

SPIE Official Online version available from SPIE Digital Library at:
https://doi.org/10.1117/12.2615068

A variable stiffness soft gripper with integrated ion-drag pump

Michael Smith, Krishna Manaswi Digumarti, Vito Cacucciolo and Herbert Shea

Soft Transducers Laboratory, École Polytechnique Fédérale de Lausanne (EPFL), Neuchâtel, Switzerland

ABSTRACT

One of the major advantages of soft grippers – the fact that they are soft - is also sometimes one of their limitations. While highly compliant materials allow these grippers to conform around and grasp objects, it also limits the amount of force that these actuators can support. Here, we present a compact, prehensile and soft gripper capable of varying its stiffness on demand, allowing not only grasping but also manipulation of objects. The gripper consists of fluidic chambers within a silicone structure and two electrostatic clutches bonded to opposite external surfaces. An integrated electrohydrodynamic pump is used to pressurize the fluidic chambers. This pump requires no moving parts, instead operating on the 'ion-drag' principle of ionizing and accelerating a dielectric liquid. As a result, these pumps are light, compact and draw only mW levels of power, allowing easy integration with the gripper to create a self-contained actuator. The gripper is actuated by pressurizing the chambers while simultaneously blocking one of the clutches, causing the structure to bend around and grasp an object. Once the object is grasped, the second clutch is blocked, increasing the bending stiffness of the structure and allowing the object to be manipulated. Furthermore, the use of this variable-stiffness configuration allows bi-directional bending using only a single pressure source. We believe our approach adds significant versatility to soft gripper applications.

1. INTRODUCTION

Soft materials are increasingly being used in the design of robots due to their inherent compliance, high flexibility, and mechanical intelligence [1]. The high degree of versatility offered by such materials make them ideal for use in robot grippers [2]. While the low stiffness of these grippers makes them attractive in the handling of flexible, delicate, and fragile objects, insufficient stiffness limits the load bearing capacity of the grippers. In this paper, we present a gripper capable of rapidly changing its stiffness.

The ability to selectively alter the stiffness is useful in grasping tasks [2], [3]. For example, a device with low stiffness can conform better to the object being picked up. However, in this state, the gripper is unable to exert forces on the object and undergoes large deformation under the forces that it is experiencing. A stiffer device can guarantee stability, exert forces, and pick up loads yet is unable to properly conform around objects. A mechanism to alter the stiffness would thus allow robot grippers to better exploit the beneficial properties of soft materials, while mitigating the inherent drawbacks.

Several techniques to transition between different stiffness states have been described in the literature on manipulators and soft robots [3], [4]. Materials that undergo a phase transition at low temperatures are a common choice. These include wax [5], low melting point alloys [6], [7], and polymers[8]–[10] to name a few. While the change in stiffness is large, the several seconds to minutes of time it takes to heat and subsequently cool the materials presents a challenge for rapid operation. Continuum manipulators which combine pneumatics with strain limiting elements in the form of cables and tendons have also been devised [11], [12]. The complexity and large size of the mechanism to control the actuators is a drawback. Another method that is commonly employed to achieve a change in stiffness is the use of jamming [13]. The central idea behind jamming is to selectively restrict motion between

loosely packed elements such as particles[14]–[17], sheets[18]–[21], or fibres [22], [23] by constricting the volume enclosing them. This is typically achieved using vacuum, under the application of which, the elements become densely packed resulting in an increase in stiffness. Devices that combine more than one type of jamming have also been used to design grippers [24]. These devices achieve a large change in stiffness but are not compact.

In this paper, we present a variable stiffness gripper in which the change in stiffness is achieved using electrostatic clutches. These clutches work on the phenomenon of electrostatic attraction between oppositely charged electrodes [25]. The clutches consist of flat electrodes separated by a dielectric. When no potential difference is applied, the electrodes are free to slide relative to each other. This is the state of low stiffness. When a voltage is applied, the electrodes attract each other, and withstand a large shear force (more than 10 N/cm^2), blocking the electrodes from sliding. Compared to the other techniques of varying stiffness, the electrostatic approach that we use has certain key advantages. The change in stiffness is near instantaneous, taking effect in the order of milliseconds. The stiffening element can also be made very thin (< 250 μm) compared to the actuator, and there is no change in volume like in the case of jamming actuators.

To function as a gripper, it is desirable to make the device capable of bending. This requires an actuator that has an antagonistic arrangement to the stiffening element. For this, a novel bellows-shaped design of connected bladders is used to create a fluidic actuator that lengthens under the application of modest pressures. Bellows-shaped bladders have previously been shown to exhibit large changes in shape [26]. In this paper, we incorporate them in a unique compact structure for a soft gripper and exploit their ability to elongate at low pressures. With the aforementioned electrostatic clutches mounted on two opposed faces, each side can be preferentially stiffened to control the direction of bending. This is different from an earlier attempt that combined dielectric elastomer actuators and electrostatic chucking to realise a bending actuator [27].

The novel actuator structure operates at relatively low pressures, so to demonstrate the utility of this design we have created an integrated system with an electrohydrodynamic (EHD) pump. EHD pumps are compact, silent and operate without any moving parts at relatively low power (of order 100 mW). While there are three different regimes of EHD pumping [28], [29]; the pump described in this work operates as an 'ion-drag' EHD pump. These pumps typically consist of asymmetrically spaced electrode pairs within a fluidic channel, and operate by applying a large DC electric field (typically several kV/mm) to ionize a dielectric fluid and accelerate the ions to the opposite electrode. The asymmetrically spaced electrodes ensure that there is a net flow of fluid along the pump. Typically EHD pumps generate tens of kPa of pressure and up to 10 ml/min of flowrate [30] [31], and find have found applications in cooling [32], [33] as well as actuation [30], [34], [35].

The variable stiffness device that we present in this paper consists of three main components. The first is a soft, inflatable silicone bladder made up of bellows-like chambers. Electrostatic clutches placed on either side of the silicone bladder to regulate its stiffness form the second component of the device. The third component is an integrated EHD pump that is used to inflate the silicone chamber. All of these components can be seen in figure 1a.

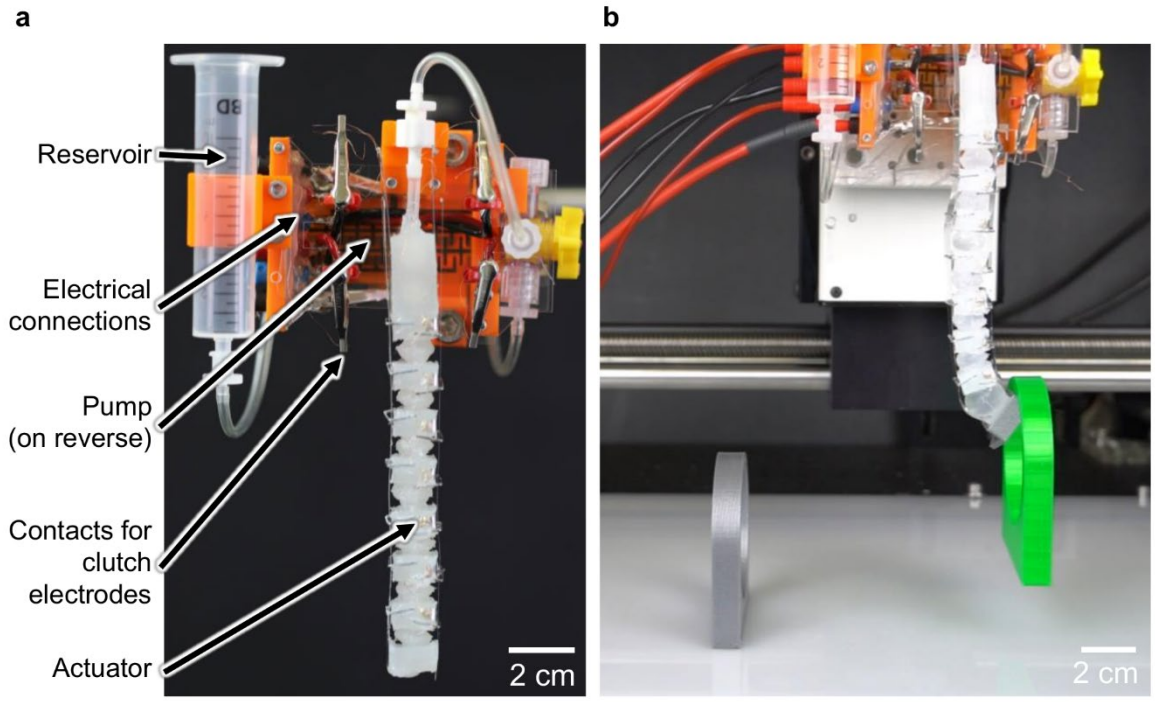

Figure 1 – a) the variable stiffness gripper with fluidic actuator, clutches, and electrohydrodynamic pump integrated into a single device**. b)** The stiffening effect of the electrostatic clutches allows the soft gripper to interact with objects.

2. MATERIALS AND METHODS

The silicone bladder was fabricated by casting uncured elastomer (Ecoflex 0030, Smooth-On) in 3D printed molds. It consists of bellow-shaped chambers alternating between flat segments (see figure 2). These pieces were cast separately. They were then loaded temporarily onto a rigid rod, aligned with respect to each other and bonded using more uncured elastomer. A silicone tube was affixed to one end of the structure using silicone glue (Silpoxy, Smooth-On) and the other end was sealed. Inserts printed in Polyethylene terephthalate glycol (PETG) with a captive nut were embedded in the silicone elastomer near the inlet. These serve as rigid mounting points for the device.

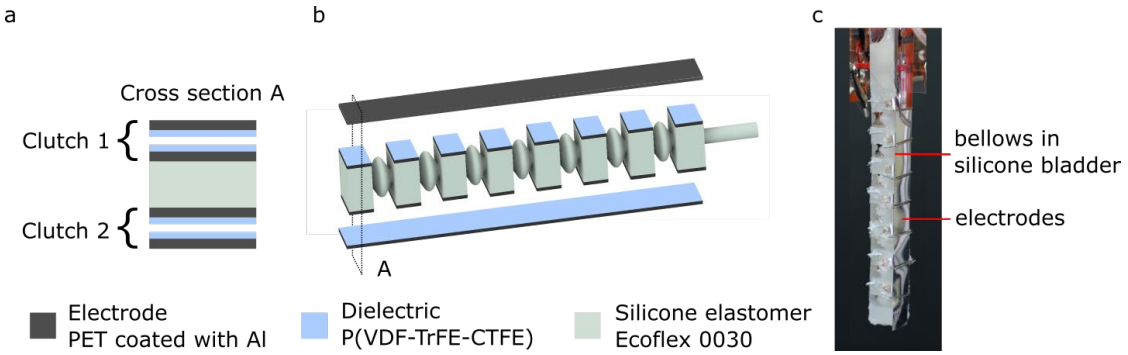

Figure 2 The components that make up the variable stiffness device. **a)** Cross sectional view of the device showing the pair of electrostatic clutches on either side of the silicone bladder. **b)** An illustration of the silicone bladder with bellows-shaped chambers and the arrangement of electrodes on its surface. **c)** A photo of the device showing its various components.

The electrodes for the electrostatic clutches were made using aluminized PET sheets (Part 7538T12, McMaster). To obtain electrodes of the desired shape, a mask made of wax was first coated onto the PET sheet in the shape of the electrode. The unmasked aluminium was etched out using 1% solution of KOH in deionized water. The wax was then removed by heating it and absorbing it out into paper. A dielectric layer of 14 wt% PVDF-TrFE-CTFE (Piezotech) in methyl ethyl ketone (Sigma Aldrich) was then coated on top of the bare aluminium. The thickness of this layer is 12.5 μm after curing in an oven at 101°C for 2 hours. To reduce friction between two electrodes sliding against each other, a 1 μm thick layer of 3 wt% thermoplastic polyurethane (MM4520, SMP) in dimethyl sulfoxide (Sigma Aldrich) is coated on top of the dielectric layer. The coated electrodes were then cut to the desired shape using a plotter (Brother SDX1200).

Electrodes of two sizes were prepared as described above. The smaller ones were affixed to the flat segments in between the bellows using silicone adhesive (Sil-poxy). The longer electrode that encompasses the entire length of the device was bonded to the silicone bladder at the tip. To keep the electrodes close to each other even when the device is in a deformed state, loops of wire were affixed to the silicone bladder at regular intervals. The space between the surfaces of the silicone structure and the wire loops is small (<1 mm) to ensure contact between the electrodes when engaged but large enough to allow sliding with minimal friction when disengaged.

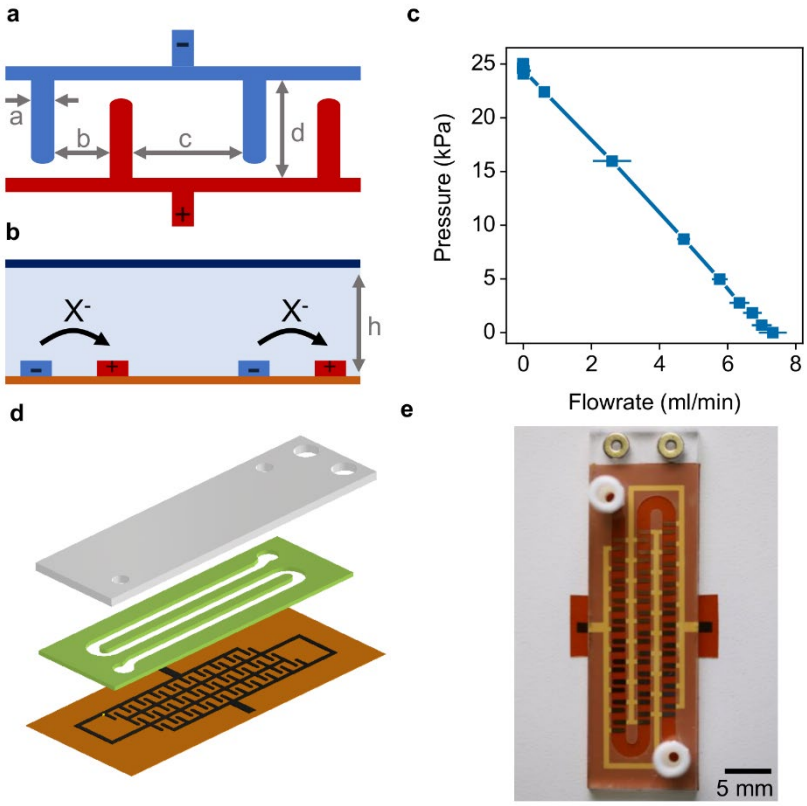

Figure 3 The EHD pumps used to power the variable stiffness gripper. **a)** The asymmetrically spaced interdigitated electrodes, indicating the parameters electrode width (*a*), electrode spacing (*b*), electrode pair spacing (*c*) and channel width (d). **b)** A cross section of the EHD pump channel, showing the negative ionisation of the fluid and acceleration toward the positive electrode. The channel height (*h*) is also marked. **c**) The characteristic 'pump curve' of these EHD pumps, acquired at a voltage of 7.2 kV (8 kV/mm), showing a maximum pressure of 25 kPa and a maximum flowrate of 7.5 ml/min. **d)** A schematic of the pump construction, showing the evaporated gold electrodes, channel spacer and pump frame**. e)** A photo of the EHD, complete with Luer-type fluidic connections.

Electrical contact between electrode segments was achieved using copper wire (75 µm diameter, Goodfellow) and conductive epoxy (CW2400, Chemtronics). Sufficient slack was provided in the wire that connects electrode segments to not restrict bending or elongation.

The EHD pumps were assembled from thermally evaporated gold electrodes, deposited through a laser cut contact mask (Nexus Tape, GP20) onto a polyimide substrate. A thin chromium adhesion layer (15 nm) was deposited first, followed by 150 nm of gold (Umicore, 99.99 %). With respect to the dimensions indicated in figure 2, the following parameters were used: a = 900 µm, b = 900 µm, c = 1.8 mm, d = 3 mm. The pump channel was formed from a spacer, laser cut from 100 um thick PET film laminated on both sides with 50 µm adhesive (ARCare, Adhesives Research), thus forming a channel height (h) of 200 um. A PMMA frame, also laser cut, was used to close the channel and to fix the Luer-lock fluidic connections. The pressure output of an EHD pump scales with the number of electrode pairs. In order to increase the pressure while minimizing the pump footprint, a serpentine arrangement of electrodes was used with 30 electrode pairs.

Throughout this work, Novec 7100 engineering fluid (3M) was used as a pumping liquid. This is a non-toxic, non-flammable fluorinated hydrocarbon with low global warming potential. The electronegativity of the fluorine groups results in the fluid molecules becoming negatively charged

when subject to a high electric field strength, thus the pumping direction is from the negative to positive electrode.

Pump curves were measured using a custom-built fluidic circuit, designed specifically to characterize the performance of EHD pumps. The setup consists of a continuous fluidic circuit containing the pump, a pressure sensor, a flowrate sensor and a motorized pinch valve. The pump curve is obtained by incrementally closing the pinch valve while simultaneously measuring the flowrate and pressure. A modified version of this fluidic circuit was used to capture pressure and flowrate values as the actuator was inflated using the EHD pump.

To measure the angle of bend of the tip when inflated at a given pressure, the device was held vertically. The end of the device near the inlet was mounted on a fixture using two screws to prevent elongation and rotation. The clutch on one side of the device was activated by applying a potential difference (350V 2Hz) across its electrodes. The clutch on the other side was left inactive and free to slide. Inflating the device results in a bend towards the side on which the clutch is active. The angle of bend of the tip with respect to the horizontal was measured at various inflation pressures. A series of pictures from such a characterization experiment are shown in figure 6 along with the pressures and the bending angles.

To measure the change in stiffness when the electrostatic clutches were engaged, the following set up was used. The device was suspended vertically from a rigid mounting plate. A hook was attached to the free end of the device. A string was connected between the hook and a pull tester (Instron 3344). As the tester moved the string, it pulled on the free end of the device. The force resisting the displacement of the device was measured on the load cell of the pull tester. A pair of adjustable pulleys was used to ensure that the pulling direction was perpendicular to the central axis in the region where the device was being pulled at. Change in stiffness is evaluated as the ratio resistive force when the clutch on one side was active to that when both the clutches were engaged. These forces were measured at a displacement of 5mm of the free end.

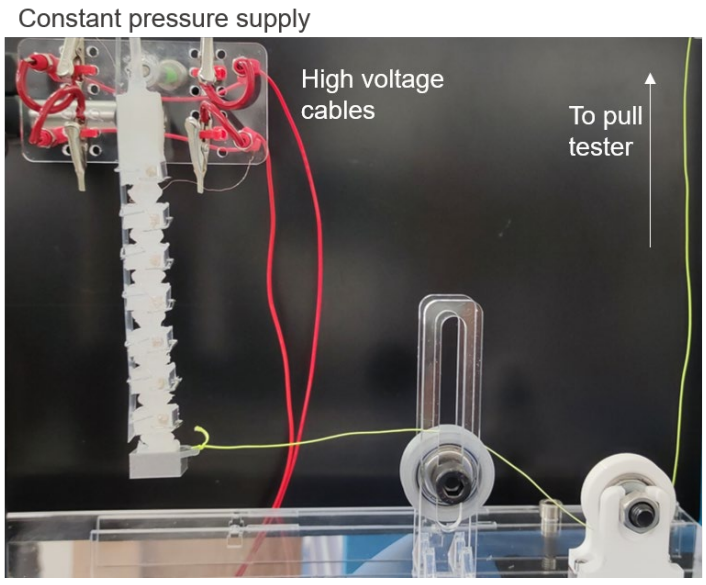

Figure 4 Experimental setup used to measure the change in stiffness of the device when the clutches are engaged. The device is suspended vertically from a fixed support. A string connected to a pull tester displaces the free end of the device while measuring the force which resists its displacement.

The fully integrated gripper consists of a mounting piece that houses the actuator, pump, fluid reservoir and all necessary electrical connections. This piece was constructed from laser cut PMMA and 3D printed PLA components. The EHD pump mounts to the rear of the device, held in place with a magnetic

coupling, while the actuator is fixed to the front of the mount via threaded inserts embedded within the silicone body. The fluidic circuit consisted of a reservoir, formed from a 10 ml syringe body, the pump, a stopcock for filling and bleeding the system, and the actuator. Six electrical connections – a pair each for the two electrostatic clutches and two for the EHD pumps, are fixed at the side of the device. All necessary fluidic connections are on-board, meaning that the gripper only requires an electrical connection. To demonstrate the gripper manipulating objects, the integrated device was mounted on a motorised three-axis gantry and used to pick up and displace two 3D printed hoops, each weighing 12 g. These tests were performed with a 2Hz 375 V clutch voltage and 7.2 kV applied to the pump.

3. RESULTS AND DISCUSSION

The geometry of the bellow-shaped chambers of the actuator determines how the structure deforms as it is inflated. To arrive at an appropriate angle for the chamber in its rest state, a simplified geometrical model was used. This is shown in figure 5. The chamber is treated to be a triangular section revolved around a central axis. Assume that the length of the slanted side (d) remains constant and that the chamber expands from an initial half-angle of α_i to a final angle half-angle of α_f. The ratio of the change in internal volume as the chamber is inflated can then be compared for designs with various initial half-angles (figure 5b). The analysis shows that this ratio reaches a peak when the chamber expands to a half-angle of 45°. It is desirable to minimise the change in internal volume to minimise the amount of fluid required to cause a change in the shape of the chamber. Designs with larger initial angles are therefore better for this reason.

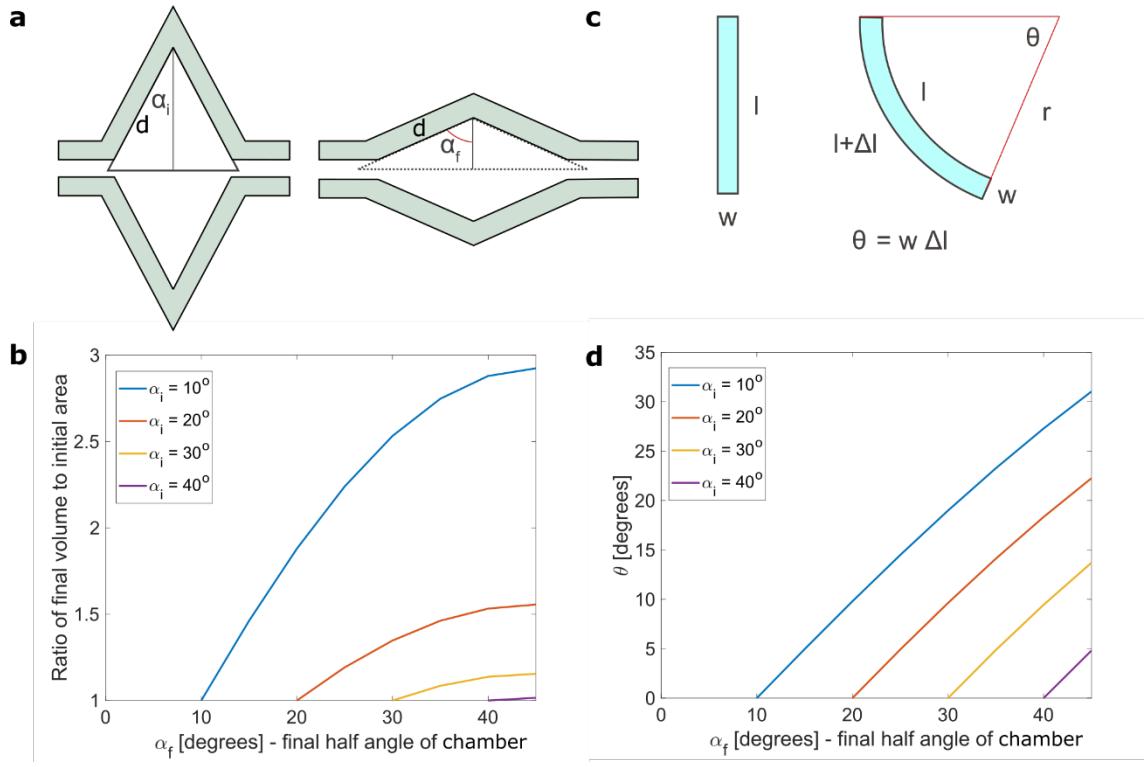

Figure 5 a) A representation of the geometric model used to analyse the elongation of a single bellows-shaped chamber. **b)** The ratio of change in volume of the chamber as a function of the final half-angle, plotted for designs with various initial half-angles. **c)** An illustration showing the relation between elongation of the device and the angle of bending when one side is held at a fixed length. **d)** The bending angle plotted as a function of final half-angle for designs with various initial half-angles.

However, the total possible elongation is reduced if the chamber starts with a larger half-angle in the rest state. The elongation of a single chamber directly affects the total elongation (and therefore the overall bending angle, figure 5c) of the device. If using chambers with larger initial half-angles (smaller possible elongation with each), a large number of chambers would be required to achieve a desired total elongation. This would increase the overall length of the device which is not desired. Chambers with a half-angle of 30^{o} in the rest state were therefore chosen to have a low change in initial volume (1.2 times) and sufficiently large elongation. In the current design with a width of 7 mm, at least 7 chambers are required to achieve a bending angle of more than 90^{o} at the tip.

Figure 6 shows the pressure response of the finalised/optimised geometry of the actuator. Two opposed sets of clutches enable bi-directional deformation, with the actuator bending towards the blocked set of electrodes. The bend angle is taken as the angle between the tip of the actuator and the horizontal, and can be seen to be symmetric with respect to pressure in each direction. The device operates between 1-15 kPa of pressure, a relatively low range for a fluidic actuator, which typically require > 50 kPa to actuate [36]–[38]. The angle of bend in this case is less than that predicted by the geometric model in figure 5. This model, however, does not consider the material properties and the non-linear elastic behavior of the elastomer. Pre-stretching of the chambers due to the weight of the lower portion of the device potentially reduces the total possible elongation.

Nonetheless, the pressure range of actuation is well matched to the performance of an EHD pump, as shown by the pressure-flowrate characteristics in figure 3c. The maximum pressure of the pump is around 25 kPa, beyond what is needed for the actuator. However, this pressure is only achieved at zero flowrate. It is more important to consider the pressure than can be generated while still maintaining a reasonable level of flow. The pump curve demonstrates that the required pressure (c. 15 kPa) can be produced at around 3 ml/min of flowrate.

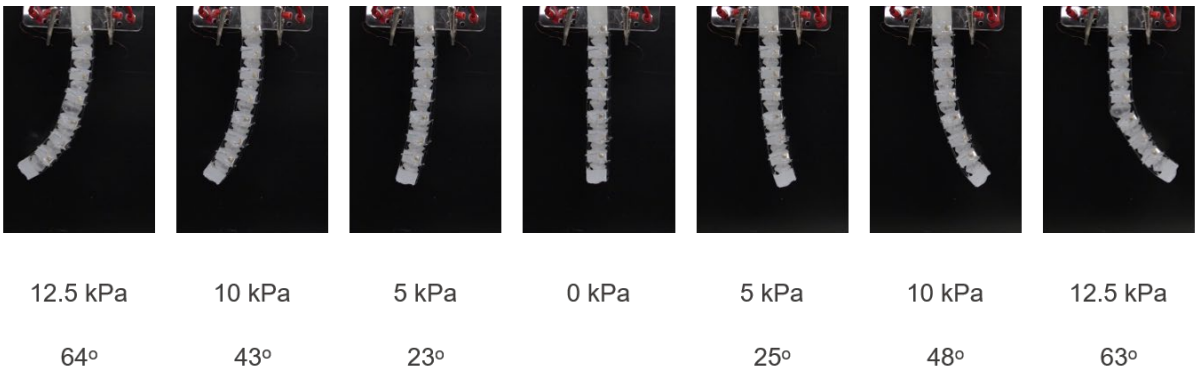

Figure 6 A series of images showing symmetric bending of the device in two opposite directions. The inflation pressures as well as the bending angles are indicated at each instance.

The dynamics of inflation and actuation are shown in figure 7. The pressure, flowrate and bend angle are shown as a function of time while the actuator is being inflated by the EHD pump. It is interesting to note that, over the timeframe require to achieve a 90-degree bend angle, the actuator inflates at a roughly constant flowrate of approximately 6 ml/min. Meanwhile, the pressure in the actuator increases and appears to saturate around 12 kPa. There is an apparent discrepancy between this behaviour and that shown in figure 3c. According to the pump curve, an increase in pressure should necessarily lead to a decrease in flowrate. However, one must also consider the elasticity of the silicone membranes as they inflate. In the case of the pump curve, the pump is working against a fixed load (a constrained channel created by a pinch valve) whereas in the case of the actuator, the load is variable. The inflating silicone chamber offers increasingly lower resistance to further inflation due to non-linear elastic behaviour of the material.

The rapid change in stiffness conferred by the use of electrostatic clutches is obvious when observing the bend angle measurements in figure 7a. The actuator transitions from fully bent to fully extended in less than a second. The degree to which the clutches stiffen the actuator can also be quantified. Stiffness was increased by a factor of 2.6±0.8 at 0 kPa of internal pressure, 3.0±0.1 at 10 kPa and 3.5±0.5 at 12.5 kPa. These values represent mean of three trials. The numbers indicate a larger stiffening ratio when in the bent state. The electrostatic clutch design presented in [39] achieves 7 times change in stiffness with four stacked clutches on each side operating at 2 kV and 3724 mm^2 of electrode overlap. In comparison, our design achieves half the change in stiffness using a single clutch on each side of the device while operating at only 375 V with an area of overlap of 390 mm^2.

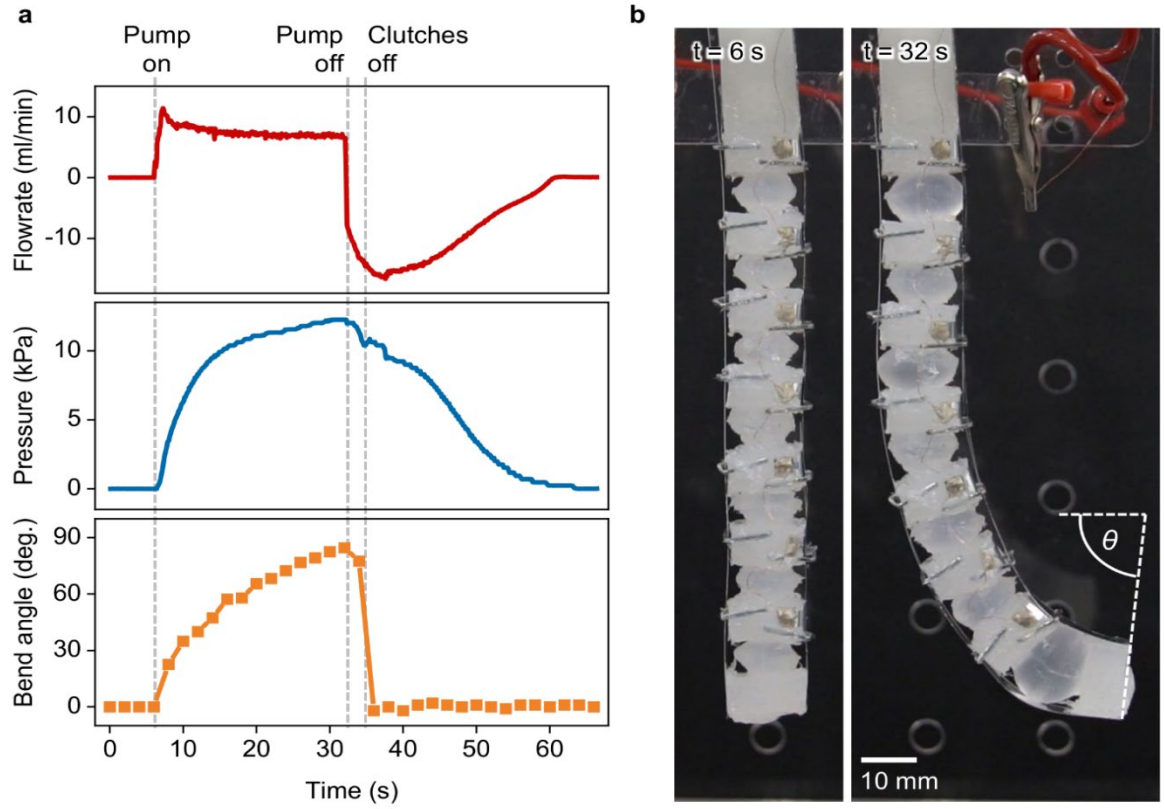

Figure 7 Dynamics of the pump-actuator system. **a)** The flowrate, pressure and bend angle as a function of time while the EHD pumps inflates the actuator. The pump voltage was 7.2 kV and the clutch voltage was 375 V at 2 Hz. A ~90 ° bend angle is achieved within 30 seconds. The data also show the rapid change in stiffness when releasing the blocked clutch. **b)** Images of the actuator before inflation and at maximum inflation. The right-hand side clutch is blocked while the left-hand side clutch is free to slide. The definition of bend angle θ is also shown. Supplementary video 1 shows the deformation of the actuator with live data: http://dx.doi.org/doi.number.goes.here.

An assembly containing the pump, fluid reservoir, actuator and all electrical connections was created to highlight how these technologies can packaged together in a compact manner, as detailed in figure 1a. The mount itself measures 80 x 60 x 25 mm, without the gripper. By integrating the pressure source with the actuator, the gripper can be entirely controlled with electrical connections, since all fluidic connections are already on-board. Figure 8 shows the gripper mounted to a motorised gantry, interacting with 3D printed objects. First the inside clutch is blocked and the EHD pump activated, inflating the actuator and causing it to be bend towards the object. Once the actuator is sufficiently deformed, the outside clutch is activated to impart some additional stiffness, allowing the actuator to lift and displace

the object. During this movement, the EHD pump remains on to maintain pressure. To release the object, both the clutches and EHD pump are turned off. The gripper rapidly loses stiffness and the object falls to the surface. The process can then be repeated, blocking the opposite clutch to bend in the opposite direction.

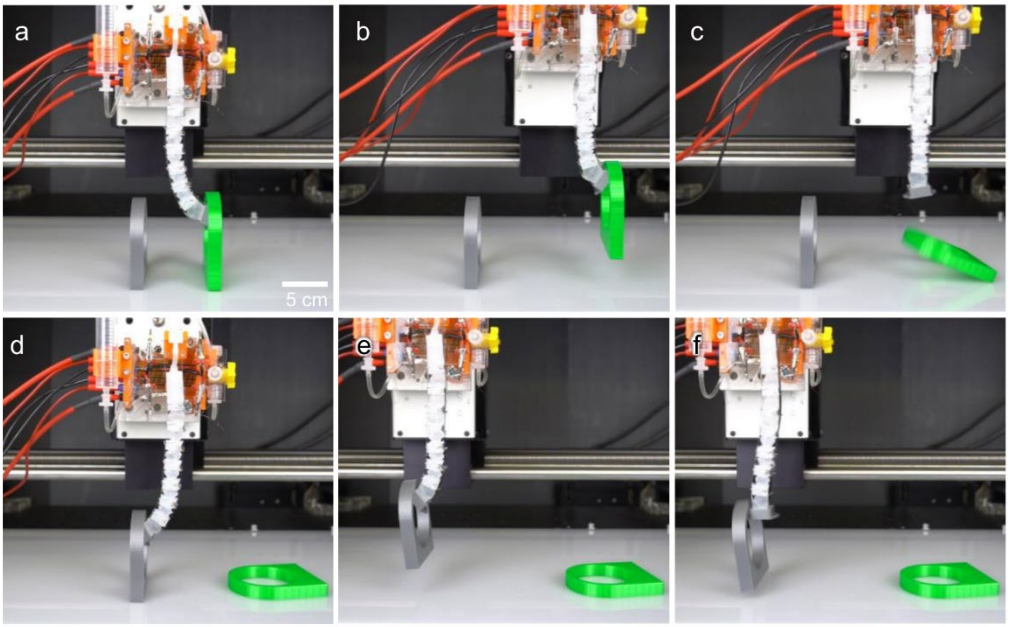

Figure 8 The integrated gripper manipulating objects; demonstrating the bidirectional bending capability (a and d), the stiffening effect of the clutches enabling an object to be lifted (b and e), and the rapid change in stiffness occurring as the clutches are turned off (c and f). Supplementary video 2 shows the entire sequence of the actuator lifting, displacing and dropping the objects: http://dx.doi.org/doi.number.goes.here.

4. CONCLUSIONS

In this work we presented a variable stiffness gripper with an integrated ion-drag EHD pump. In using electrostatic clutches as the stiffening element of the actuator, we are able to achieve up to a 3.5x increase in flexural rigidity within milliseconds. This is the case with both stiffening and softening the device, a particularly useful advantage when compared to other methods of changing stiffness. Furthermore, the use of two opposed clutches allows bi-directional bending with a single pressure source and with no requirements for valves. The novel segmented bellows-shaped actuator design allows inflation and bending at relatively low pressures, around 12-15 kPa, enabling the use of an integrated ion-drag EHD pump as a pressure source. The integrated design (measuring 60 x 80 x 25 mm) with the EHD pump, silicone structure and the electrostatic clutches demonstrates the compact nature of the device. Since all the fluidic components are already integrated, our system only requires electrical cables for both operation and control.

The performance of the device can be improved in terms of the ratio of the change in stiffness. Potential means to achieve this are using multiple layers of clutches and operating at higher voltages. The clutches are good at resisting tensile loads but buckle under compressive loads. Modifications to the manner in which the clutches are integrated on to the silicone structure will look at addressing this issue in the future. Combining several units of the device presented here to achieve multi-directional bending is another potential extension of the current work.

5. ACKNOWLEDGMENT

KMD and MS contributed equally to the work. KMD has received funding from the European Union's Horizon 2020 research and innovation programme under grant agreement No 869963 (MERGING). MS received funding from the Swiss National Science Foundation SNF project number IZLJZ2_183656.

6. REFERENCES

[1] S. Kim, C. Laschi, and B. Trimmer, 'Soft robotics: a bioinspired evolution in robotics', *Trends in biotechnology*, vol. 31, no. 5, pp. 287–294, 2013, doi: 10/gbcz3x.
[2] J. Shintake, V. Cacucciolo, D. Floreano, and H. Shea, 'Soft robotic grippers', *Advanced Materials*, vol. 30, no. 29, p. 1707035, 2018, doi: 10/gdhj9b.
[3] M. Manti, V. Cacucciolo, and M. Cianchetti, 'Stiffening in Soft Robotics: A Review of the State of the Art', *IEEE Robotics Automation Magazine*, vol. 23, no. 3, pp. 93–106, Sep. 2016, doi: 10/gd52dm.
[4] L. Blanc, A. Delchambre, and P. Lambert, 'Flexible medical devices: Review of controllable stiffness solutions', in *Actuators*, 2017, vol. 6, no. 3, p. 23. doi: 10/ggrhg9.
[5] N. G. Cheng, A. Gopinath, L. Wang, K. Iagnemma, and A. E. Hosoi, 'Thermally tunable, self-healing composites for soft robotic applications', *Macromolecular Materials and Engineering*, vol. 299, no. 11, pp. 1279–1284, 2014, doi: 10/f2swd4.
[6] J. Shintake, B. Schubert, S. Rosset, H. Shea, and D. Floreano, 'Variable stiffness actuator for soft robotics using dielectric elastomer and low-melting-point alloy', in *2015 IEEE/RSJ International Conference on Intelligent Robots and Systems (IROS)*, 2015, pp. 1097–1102. doi: 10/gmvz3x.
[7] A. Tonazzini, S. Mintchev, B. Schubert, B. Mazzolai, J. Shintake, and D. Floreano, 'Variable stiffness fiber with self-healing capability', *Advanced Materials*, vol. 28, no. 46, pp. 10142–10148, 2016.
[8] A. M. Nasab, A. Sabzehzar, M. Tatari, C. Majidi, and W. Shan, 'A soft gripper with rigidity tunable elastomer strips as ligaments', *Soft robotics*, vol. 4, no. 4, pp. 411–420, 2017, doi: 10/gdghht.
[9] A. Firouzeh, M. Salerno, and J. Paik, 'Stiffness control with shape memory polymer in underactuated robotic origamis', *IEEE Transactions on Robotics*, vol. 33, no. 4, pp. 765–777, 2017, doi: 10/gbsp7m.
[10] B. Aksoy and H. Shea, 'Dynamically reconfigurable DEAs incorporating shape memory polymer fibers', in *Electroactive Polymer Actuators and Devices (EAPAD) XXI*, 2019, vol. 10966, p. 109661Y. doi: 10/gn9thf.
[11] G. Immega and K. Antonelli, 'The KSI tentacle manipulator', in *Proceedings of 1995 IEEE international conference on robotics and automation*, 1995, vol. 3, pp. 3149–3154. doi: 10/d2zcsf.
[12] A. Stilli, H. A. Wurdemann, and K. Althoefer, 'Shrinkable, stiffness-controllable soft manipulator based on a bio-inspired antagonistic actuation principle', in *2014 IEEE/RSJ International Conference on Intelligent Robots and Systems*, 2014, pp. 2476–2481. doi: 10/gmvz4w.
[13] S. G. Fitzgerald, G. W. Delaney, and D. Howard, 'A Review of Jamming Actuation in Soft Robotics', in *Actuators*, 2020, vol. 9, no. 4, p. 104. doi: 10/gmvzz7.
[14] V. Wall, R. Deimel, and O. Brock, 'Selective stiffening of soft actuators based on jamming', in *2015 IEEE International Conference on Robotics and Automation (ICRA)*, 2015, pp. 252–257. doi: 10/gjm6bm.
[15] T. Ranzani, G. Gerboni, M. Cianchetti, and A. Menciassi, 'A bioinspired soft manipulator for minimally invasive surgery', *Bioinspiration & biomimetics*, vol. 10, no. 3, p. 035008, 2015, doi: 10.1088/1748-3190/10/3/035008.
[16] M. Cianchetti, T. Ranzani, G. Gerboni, I. De Falco, C. Laschi, and A. Menciassi, 'STIFF-FLOP surgical manipulator: Mechanical design and experimental characterization of the single module', in *2013 IEEE/RSJ international conference on intelligent robots and systems*, 2013, pp. 3576–3581. doi: 10/ghbtw7.

[17] S. Hauser, M. Robertson, A. Ijspeert, and J. Paik, 'Jammjoint: A variable stiffness device based on granular jamming for wearable joint support', *IEEE Robotics and Automation Letters*, vol. 2, no. 2, pp. 849–855, 2017, doi: 10/gmvz2g.
[18] Y.-J. Kim, S. Cheng, S. Kim, and K. Iagnemma, 'Design of a tubular snake-like manipulator with stiffening capability by layer jamming', in *2012 IEEE/RSJ International Conference on Intelligent Robots and Systems*, 2012, pp. 4251–4256. doi: 10/f2395j.
[19] Y.-J. Kim, S. Cheng, S. Kim, and K. Iagnemma, 'A novel layer jamming mechanism with tunable stiffness capability for minimally invasive surgery', *IEEE Transactions on Robotics*, vol. 29, no. 4, pp. 1031–1042, 2013, doi: 10/f23zdx.
[20] J. Ou, L. Yao, D. Tauber, J. Steimle, R. Niiyama, and H. Ishii, 'jamSheets: thin interfaces with tunable stiffness enabled by layer jamming', in *Proceedings of the 8th International Conference on Tangible, Embedded and Embodied Interaction*, 2014, pp. 65–72.
[21] Y. S. Narang, J. J. Vlassak, and R. D. Howe, 'Mechanically versatile soft machines through laminar jamming', *Advanced Functional Materials*, vol. 28, no. 17, p. 1707136, 2018, doi: 10/gmvzzm.
[22] M. Brancadoro, M. Manti, S. Tognarelli, and M. Cianchetti, 'Preliminary experimental study on variable stiffness structures based on fiber jamming for soft robots', in *2018 IEEE International Conference on Soft Robotics (RoboSoft)*, 2018, pp. 258–263. doi: 10/gmvzzj.
[23] N. Vasios, Y. Narang, B. Aktaş, R. Howe, and K. Bertoldi, 'Numerical analysis of periodic laminar and fibrous media undergoing a jamming transition', *European Journal of Mechanics-A/Solids*, vol. 75, pp. 322–329, 2019, doi: 10/gmvz43.
[24] Y. Yang, Y. Zhang, Z. Kan, J. Zeng, and M. Y. Wang, 'Hybrid jamming for bioinspired soft robotic fingers', *Soft robotics*, vol. 7, no. 3, pp. 292–308, 2020, doi: 10/gh7zxh.
[25] 'High Force Density Textile Electrostatic Clutch - Hinchet - 2020 - Advanced Materials Technologies - Wiley Online Library'. https://onlinelibrary.wiley.com/doi/abs/10.1002/admt.201900895 (accessed Jan. 27, 2022).
[26] K. M. Digumarti, A. T. Conn, and J. Rossiter, 'Euglenoid-Inspired Giant Shape Change for Highly Deformable Soft Robots', *IEEE Robotics and Automation Letters*, vol. 2, no. 4, pp. 2302–2307, Oct. 2017, doi: 10/gn9vrf.
[27] H. Imamura, K. Kadooka, and M. Taya, 'A variable stiffness dielectric elastomer actuator based on electrostatic chucking', *Soft matter*, vol. 13, no. 18, pp. 3440–3448, 2017, doi: 10/f97dnw.
[28] A. Ramos, Ed., *Electrokinetics and Electrohydrodynamics in Microsystems*. Vienna: Springer Vienna, 2011. doi: 10.1007/978-3-7091-0900-7.
[29] J. Seyed-Yagoobi, 'Electrohydrodynamic pumping of dielectric liquids', *Journal of Electrostatics*, vol. 63, no. 6, pp. 861–869, Jun. 2005, doi: 10/bnjt4r.
[30] V. Cacucciolo, J. Shintake, Y. Kuwajima, S. Maeda, D. Floreano, and H. Shea, 'Stretchable pumps for soft machines', *Nature*, vol. 572, no. 7770, pp. 516–519, Aug. 2019, doi: 10.1038/s41586-019-1479-6.
[31] J. W. Kim, T. Suzuki, S. Yokota, and K. Edamura, 'Tube-type micropump by using electro-conjugated fluid (ECF)', *Sensors and Actuators, A: Physical*, vol. 174, no. 1, pp. 155–161, 2012, doi: 10.1016/j.sna.2011.10.027.
[32] J. Darabi and H. Wang, 'Development of an electrohydrodynamic injection micropump and its potential application in pumping fluids in cryogenic cooling systems', *Journal of Microelectromechanical Systems*, vol. 14, no. 4, pp. 747–755, 2005, doi: 10.1109/JMEMS.2005.845413.
[33] N. V. Tobar, P. N. Christidis, N. J. O'Connor, M. Talmor, and J. Seyed-Yagoobi, 'Experimental Study of Flexible Electrohydrodynamic Conduction Pumping for Electronics Cooling', in *ASME 2018 International Technical Conference and Exhibition on Packaging and Integration of Electronic and Photonic Microsystems*, Aug. 2018, no. February. doi: 10.1115/IPACK2018-8322.
[34] V. Cacucciolo, H. Nabae, K. Suzumori, and H. Shea, 'Electrically-Driven Soft Fluidic Actuators Combining Stretchable Pumps With Thin McKibben Muscles', *Frontiers in Robotics and AI*, vol. 6, no. January, pp. 1–8, Jan. 2020, doi: 10.3389/frobt.2019.00146.
[35] Z. Mao, T. Iizuka, and S. Maeda, 'Bidirectional electrohydrodynamic pump with high symmetrical performance and its application to a tube actuator', *Sensors and Actuators A: Physical*, vol. 332, p. 113168, Dec. 2021, doi: 10.1016/j.sna.2021.113168.

[36] A. Pagoli, F. Chapelle, J. A. Corrales Ramón, Y. Mezouar, and Y. Lapusta, ‘Review of Soft Fluidic Actuators: Classification and Materials Modeling Analysis’, *Smart Mater. Struct.*, Nov. 2021, doi: 10/gngvr3.
[37] P. Polygerinos *et al.*, ‘Soft Robotics: Review of Fluid-Driven Intrinsically Soft Devices; Manufacturing, Sensing, Control, and Applications in Human-Robot Interaction’, *Advanced Engineering Materials*, vol. 19, no. 12, p. 1700016, 2017, doi: 10/gd52dk.
[38] F. Connolly, P. Polygerinos, C. J. Walsh, and K. Bertoldi, ‘Mechanical Programming of Soft Actuators by Varying Fiber Angle’, *Soft Robotics*, vol. 2, no. 1, pp. 26–32, Mar. 2015, doi: 10/f7xp87.
[39] T. Wang, J. Zhang, Y. Li, J. Hong, and M. Y. Wang, ‘Electrostatic layer jamming variable stiffness for soft robotics’, *IEEE/ASME Transactions on Mechatronics*, vol. 24, no. 2, pp. 424–433, 2019, doi: 10/gmvzzk.